IFMIF-LIPAc DIAGNOSTICS AND ITS CHALLENGES

J. Marroncle, P. Abbon, J.F. Denis, J. Egberts, F. Jeanneau, J.F. Gournay, A. Marchix, J.P. Mols, T. Papaevangelou, M. Pomorski, CEA Saclay, France
J. Calvo, J.M. Carmona, P. Fernández, A. Guirao, D. Iglesias, C. Oliver, I. Podadera, A. Soleto, CIEMAT Madrid, Spain
M. Poggi, INFN Legnaro, Italy

Abstract

The International Fusion Materials Irradiation Facility (IFMIF) aims at providing a very intense neutron source (10^{17} neutron/s) to test the structure materials for the future fusion reactors beyond ITER (International Thermonuclear Experimental Reactor). Such a source will be driven using 2 deuteron accelerators of 125 mA cw each up to 40 MeV impinging into a lithium liquid curtain, thus producing very high neutron flux with a similar spectrum as those expected in fusion reactors. A validation phase was decided for this 10 MW facility consisting in the construction of part of the accelerator facility, the so-called LIPAc (Linear IFMIF Prototype Accelerator).

LIPAc, which is in construction phase, will accelerate a 125 mA cw beam deuteron up to the first of the four superconductive modules foreseen for IFMIF. The 9 MeV beam will be driven through the HEBT to the beam dump. This facility is currently under construction at Rokkasho (Japan).

In this contribution, we describe the beam diagnostics foreseen for this 1.125 MW prototype accelerator emphasizing the challenges encountered and present solutions how to overcome them.

IFMIF-EVEDA

The International Fusion Materials Irradiation Facility (IFMIF) [1], a project involving Japan and Europe in the framework of the "Broader Approach", aims at producing an intense flux of neutrons, in order to characterize materials envisaged for future fusion reactors. That should be done with 2 deuteron beam accelerators (125 mA - 40 MeV) impinging a liquid lithium target, producing a huge neutron flux (10^{17} neutrons/s) [2]. Downstream to this huge neutron source, cells will be implemented to test the responses of material samples submitted to mechanical and thermal stresses in these very harsh conditions.

Such a powerful 10 MW facility, sketched in Fig. 1, poses unprecedented challenges. Therefore, it was decided to perform a validation phase, EVEDA (Engineering Validation and Engineering Design Activities) consisting of designing and manufacturing a prototype accelerator, a 1/3-scaled Li loop target and part of test cells.

The LIPAc accelerator prototype (Linear IFMIF Prototype Accelerator) [3] is in designing and manufacturing phases; it will be installed at Rokkasho (Japan). LIPAc will accelerate 125 mA of deuterons up to 9 MeV. It is a 1-scaled IFMIF accelerator up to the first accelerating cryomodule. The huge space charge effect is a major challenge at this very high power beam (1.125 MW), which is particularly tricky for the beam transportation at low energy.

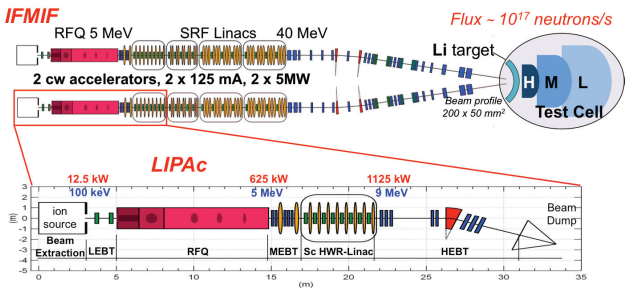

Figure 1: IFMIF facility (top) and LIPAc (bottom) [4].

In this paper, we will introduce a few challenges that LIPAc has to cope with as well as their impact on diagnostics. Then, a quick diagnostic overview will be given before to focus on the most challenging one.

IFMIF & LIPAc CHALLENGES

D^+ particles will be accelerated firstly by the source extraction system up to 100 keV [5] and then injected into the RFQ. At the RFQ exit [6], the 125 mA cw beam is bunched at 175 MHz with deuteron energy of 5 MeV. The first accelerating cryomodule (Superconductive Radio Frequency Linac or SRF Linac) with its half wave resonators (HWR) will give a last kick to reach the final LIPAc energy of 9 MeV [7]. Up to here, both LIPAc and IFMIF accelerators are identical. For IFMIF, three additional accelerating cryomodules will be added to reach 40 MeV.

Figure 2 [4] summarize the average beam power versus the beam energy for various linear facilities showing that IFMIF is the most powerful accelerator at given beam energy.

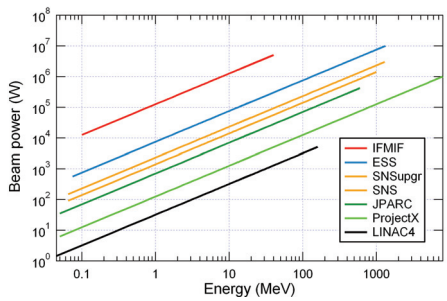

Figure 2: Average beam power for various linear facilities versus beam energy.

ISBN 978-3-95450-119-9

This high beam power results in a very high space Charge. Beam dynamics use the generalized perveance K, which is the relevant parameter depicting the SC forces.

$$K = {}^{qI}/_{2\pi\varepsilon_0 m_0 \gamma^3 v^3},$$

with ε_0 being the vacuum permittivity, I the beam intensity, γ the relativistic factor and m_0, q, v being the particle rest mass, charge and speed, respectively.

The generalized perveance is presented on Fig. 3 [4] versus the beam energy for the same facilities.

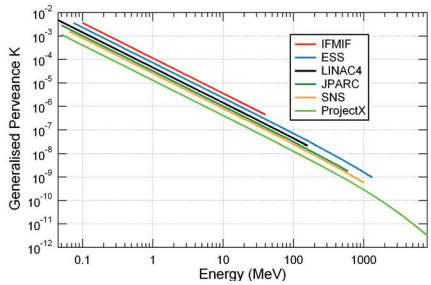

Figure 3: Generalized perveance for various linear facilities versus beam energy.

As expected, this figure shows that SC is the strongest for IFMIF & LIPAc beams. In term of accelerating structures, a direct consequence is the worldwide longest RFQ ever constructed. Indeed, as the SC effect decreases with beam energy, particles have to be accelerated highly enough in the RFQ to be injected and accelerated efficiently in the SRF Linac. To illustrate the SC effect, Fig. 3 exhibits a same perveance for IFMIF at 5 MeV (RFQ output energy) as for LINAC4 around 2.7 MeV (RFQ output energy is 3 MeV).

Main consequences of the high power and SC of IFMIF / LIPAc beams are listed below:

- Very compact beam line to prevent the beam from exploding under SC forces implying lack of space for diagnostics, particularly on LEBT and MEBT.
- For injector and RFQ, beam losses are still significant (few % of the beam) implying issues to get the 125 mA nominal beam intensity
- For MEBT, SRF Linac and HEBT, losses induce harmful material activation and must be kept well below 1 W/m which is a very tiny fraction of the total beam power
- Low beam energy have also negative effects like:
  - Low β (β<0.1) leading to bunch overlapping (far from plane wave hypothesis) or beam de-bunching
  - Very high and dense deposit of energy into interceptive monitors (material vaporization)
  - Only neutral secondary particles exit from the beam pipe for which monitor sensitivity is quite poor (beam losses…)

All these issues had to be taken into account while designing LIPAc diagnostics.

Radiation Background

High radiation background levels are another LIPAc challenge. Indeed the Beam Dump (BD) [8] is designed to cope with a 1.125 MW beam power. A large amount of particles, gammas (γ) but mainly neutrons, are backscattered in the beam direction. The dipole that deviates the beam by 20° downstream the diagnostic plate prevents these neutrons from irradiating the entire beam line. Anyway, even though major LIPAc components (upstream the dipole) are protected from these particles, they induce a very large background into the accelerator vault, particularly in the vicinity of the BD. A shielding strategy based on polyethylene plates (CH_2) is in validation phase. As sketched in Fig. 4, 2 CH_2 walls located against the concrete wall of the BD, topped with a CH_2 roof as a tunnel, act to confine radiation. A V-shape CH_2 block is also installed to absorb remaining backscattered particles. Only the effect due to neutrons coming from the BD is shown here, which is the very most dominant.

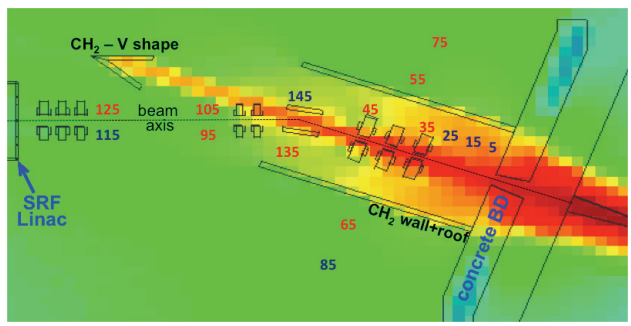

Figure 4: Neutron background in the downstream part of LIPAc. Polyethylene wall and V shape wall are shown.

Table 1: Half-year Neutron Fluences at Various Locations

Point #	5	25	145	115	85
n/cm²/s	7×10^{8}	5×10^{8}	4×10^{7}	6×10^{6}	4×10^{6}
Fluence	1×10^{16}	8×10^{15}	6×10^{14}	9×10^{13}	7×10^{13}

Neutron fluences calculated in the horizontal beam plane for 6 months cw beam are given in Table 1 for various locations referred in Fig. 4.

It was observed in electronic laboratory at CEA Saclay [9] that failures on some electronics may appear for neutron fluences greater than 10^{11} n/cm² at neutron energies around 1 MeV. Fluences in the LIPAc vault are largely higher than this value, even far from the beam dump, therefore peculiar caution for material choice need to be done and electronics will be put outside of the vault. Fortunately, LIPAc operation will be mostly done in pulsed beam concerning commissioning.

LIPAc DIAGNOSTIC OVERVIEW

LIPAc is shown in Fig. 5 with all its diagnostics, which can be divided in 2 parts:

Diagnostics for the Injector

The ECR source (2.45 GHz) produces and accelerates D^+ up to 100 keV, which are then transported through the LEBT and finally injected into the RFQ. The LEBT is

ISBN 978-3-95450-119-9

made of two solenoids and a cross-line where viewports allow diagnostics insertion as well as a fast chopper.

- Low Emittance: it is measured with an Allison scanner that is supposed to work in cw mode. Thus it is designed for sustaining a 15 kW beam power.
- Species fractions are measured using a Doppler technique i.e. a spectrometer is set in a shielding area remotely plugged to the pipe chamber via a fiberscope [10].
- 4 grids analyzer to measure the space charge.
- A Faraday Cup for beam current measurement.

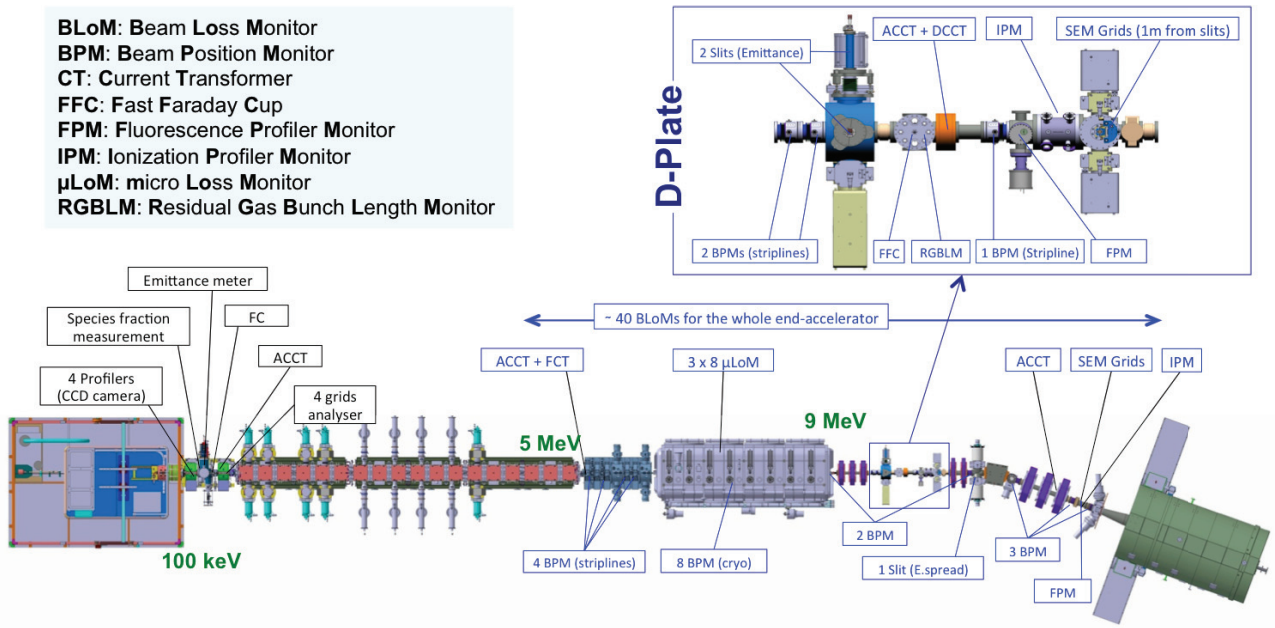

Figure 5: LIPAc diagnostics overview.

- An ACCT (Alternating Current) is set around the cone located upstream to the RFQ. It will provide the RFQ transmission in pulsed mode by comparison with the MEBT ACCT.
- CID cameras (Charge Injection Device) for beam induced profile measurement. CID is a radiation hard device wrt normal cameras.
- Thermocouples on electrodes are also foreseen.

For the injector [11] commissioning, a specific diagnostic plate is foreseen that will be used only during this phase.

Diagnostics Downstream the RFQ

The Diagnostic Plate (DP) is a movable device which integrates all the diagnostics set required for the beam characterization and tuning during the different commissioning phases and the accelerator nominal operation (see Fig. 5). The DP will be installed firstly downstream the MEBT for the RFQ commissioning and will be moved later on to its final location, i.e. downstream to the SRF Linac, in the HEBT.

The diagnostics that will be installed after the RFQ (which includes MEBT, SRF linac and HEBT) are summarized below:

- Current Transformer: due to lack of space, an ACCT will be set in the MEBT downstream to the RFQ for its transmission measurement. It will share its frame with a Fast CT (large Band Width) resolving single bunches to insure that the beam is passing through in cw mode. One DCCT will be set in the D-Plate for cw current measurement.
- BPM: various types, button and stripline, at room and cryogenic temperature. Energy measurement is done in the D-Plate with the three stripline-type BPMs.
- Profilers:
  - Interceptive: SEM grids for emittance measurement and energy spread at very low duty cycle [12],
  - Non-interceptive: two types are foreseen, both based on residual gas beam interaction, one on fluorescence and one on ionization.
- Bunch length:
  - Interceptive: Fast Faraday Cup,
  - Non-interceptive: based on residual gas ionization; the ionized products, electrons or ions, are extracted and sorted in energy filtered in a magnetic field before their detection on a MCP. Therefore, electron time of flight versus RF phase gives access to bunch time shape.
- Slits are used for emittance and dipole dispersion measurements (energy spread).
- Beam losses:
  - LHC-type Ion Chambers will be used as BLoM,
  - Diamond detectors will be implemented into the cryomodule to perform measurements of

ISBN 978-3-95450-119-9

small beam losses in order to fine-tune the machine.

DESCRIPTION OF MOST CHALLENGING DIAGNOSTICS

In this section, some diagnostics will be presented in more detail. They are selected for their challenging sides but not all of them will be described in detail.

Allison Scanner

An Allison scanner was developed at CEA Saclay to measure the emittance of the source in cw mode. Thus, the objective is to sustain a power deposit of 15 kW. The emittance monitor was designed after thermal studies using COMSOL [13]. The entrance slits of 100 µm aperture and 17 cm length are made of a thick copper radiator longitudinally drilled with 20 channels to flow water at high pressure for cooling. Thick layers of tungsten (5 mm) are brazed on copper to avoid copper fusion. The entire system, including thermal shielding, electric deviation electrodes, Faraday cup… occupies a 16×14×17 cm^3 volume. Finally, the Allison scanner is mounted on a translator allowing its insertion or removal from the beam. It is in commissioning progress on the LIPAc LEBT installed at Saclay for commissioning, too. To avoid injector activation before transportation to Japan, the emittance has been measured only with proton beams up to now. Such an experimental emittance measurement is presented in Fig. 6 (right) for a cw proton beam of 81 mA and 50 keV (4 kW).

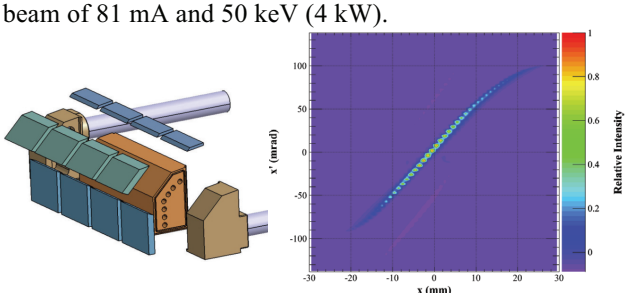

Figure 6: Half part of the slit with the copper plate (brown), the tungsten tiles (blue) and the water inlet on left figure. Experimental emittance measurement in (x,x') plane done with a 4 kW proton LIPAc beam (right).

From this plot, the extracted experimental emittance (proton) is ε_{rms}=0.29 π.mm.mrad close to the deuteron RFQ acceptance value 0.30 π.mm.mrad. Emittance for deuteron should be better.

Non-interceptive Profiler

Non-interceptive profile monitors are critical devices for our project, particularly for IFMIF. Indeed, the interaction of both beams with the lithium target needs to be well monitored to avoid problems like Li boiling. The target proximity implies lots of backscattered particles (neutrons, γ), thus generating a very harsh radioactive background, an ionized Li based vacuum as well as secondary reactions on the profiler structure itself. The beam intercept size is 5x20 cm^2 requiring severe beam position and shape stabilities. Such difficulties have motivated the construction of two types of profilers for LIPAc, both based on residual gas beam interactions: fluorescence and ionization.

Ionization Profile Monitor (IPM)

The IPM [14] should be able to measure the transverse profile of the beam for deuteron energy ranging from 5 to 9 MeV, in cw beam or pulsed mode, with a resolution of around 1 mm at 125 mA. Two IPMs are required:

- On the D-Plate, where 6σ beam diameter is around 5 cm and pressure ~10^{-7} mbar,
- Upstream the Beam Dump (BD), where 6σ beam diameter is around 8 cm and pressure ~10^{-5} mbar.

A first prototype with a 6×6 cm^2 aperture and 4 cm depth was designed. An electric field is applied between 2 parallel plates: HV (~5 kV) on one while 32 conductive strips (4×3 cm^2) are printed on the grounded electrode. On each side of the active area 6 thin pads (degraders) are set at specific voltages to reduce fringe fields. The voltages are applied over a resistor chain (typically 50 MΩ). The resistor values were thoroughly chosen by optimizing the electric field homogeneity. A complete electric field study was done using electromagnetic software packages to solve Poisson's equation, like Lorentz [15]. During a first test campaign performed at GSI, on the X2 line of the UNILAC, following results were observed:

- Electric field uniformity: checked by comparing the IPM position, moved precisely with a stepper motor, to the reconstructed central profile position. Very good linearity was achieved as shown on Fig. 7 (left).
- Profile position resolution: profiles are measured every 2 µs, then the rms of the profile centers is calculated by integrating over time. In Fig. 7 (right), σ (rms)~100 µm is reached (I=120µA – Xe^{21+} beam) for integration time larger than 0.2 ms.

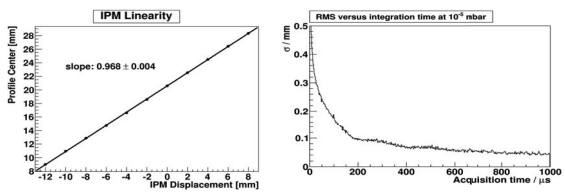

Figure 7: IPM linearity (left) and resolution (right).

- Profile comparison IPM / GSI-FPM: using a FPM developed at GSI, comparisons for various residual were done.

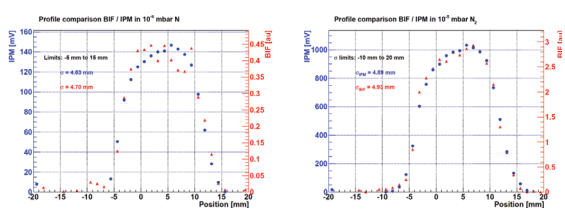

Figure 8: IPM / GSI FPM profile comparisons.

ISBN 978-3-95450-119-9

Figure 8 shows very nice agreement between IPM (blue) and FPM (red) profiles; N_2 residual gas pressure was 10^{-6} mbar (left) and 10^{-5} mbar (right).

- Signal extrapolation data: such an IPM should be able measuring LIPAc beam profile down to 4.2 mA in residual gas pressure > 10^{-7} mbar when GSI parameters are scaled to LIPAc ones.

A first projection of the upstream BD IPM (Fig. 9-left) was then designed and tested. At least the 3 following issues are identified:

- Axial lack of space combined with the large IPM aperture (15×15 cm^2) affects the electric field uniformity. Extra degraders are then implemented for optimization,
- High radiation level (~7 kSv/h neutron and 12 Sv/h for γ in the beam axis): radiation hard materials are used like stainless steel, ceramics, copper, indium joints, epoxy.
- Large space charge effect: even with a 20 kV applied between field electrodes, space charge effects still remain. An algorithm was developed [16] to correct measured data. It was tested successfully on the CEA Saclay high intensity proton source (SILHI [17]). The 90 keV beam conditions were kept constant while the IPM extraction voltages were varied leading to different profiles (blue profiles on Fig. 9-right, larger profiles corresponding to lower HVs). The corrected profiles (red) for each of them match very well, giving confidence in the algorithm method.

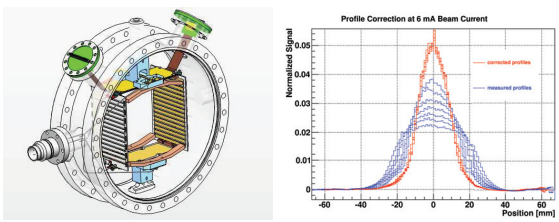

Figure 9: Beam Dump IPM drawing (left) and space charge algorithm correction (right).

Fluorescence Profile Monitor (FPM)

The high beam current of LIPAc should be favorable to measure transverse profile using beam induced fluorescence. Experimental tests with a 9 MeV deuteron beam were done to demonstrate the feasibility of FPMs for LIPAc using two different prototypes. One is based on a linear multi-anode PMT array, whereas the other is based on a custom intensified CID (Charge Injection Device) camera designed at CIEMAT Madrid [18].

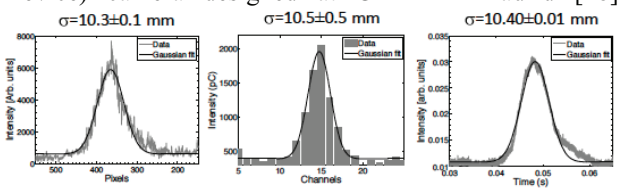

Figure 10: CID, PMT and wire scanner beam profile crosschecks [18].

Both prototypes were tested in two different campaigns with a 9 MeV deuteron beam delivered by the cyclotron of the Centro Nacional de Aceleradores at Sevilla (Spain), at currents up to a few tens of µA. During the first campaign, cross-checks between FPMs and a wire scanner, systematic beam current and vacuum pressure scans as well as tests using different working gas (N_2, Xe, Ar and Ne) were performed. As shown on Fig. 10, profiles obtained with CID (left), PMT (center) and a wire scanner (right) were in good agreement for a 15 µA deuteron current in 7.10^{-4} mbar residual gas: Gaussian fit gives respectively the σ (mm) values 10.3±0.1, 10.5±0.5 and 10.40±0.10 respectively.

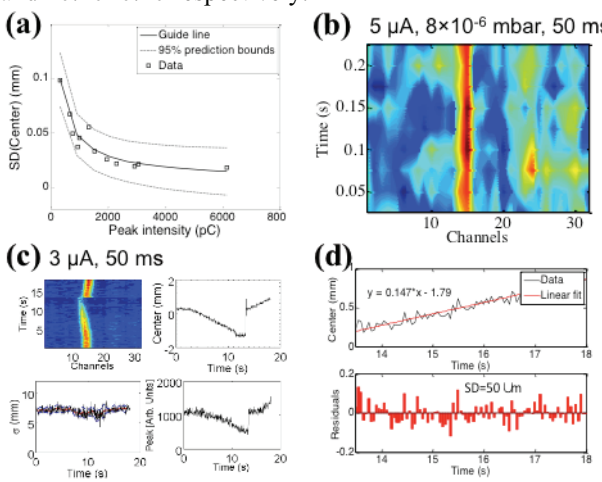

Figure 11: Beam position resolutions achieved during first campaign (a). A beam profile evolution (b), a beam steering experiment (c) and an analysis of the beam position resolution (d) achieved (50 µm) for a steered beam recorded during the second campaign are shown.

A second campaign served as optimization: (a) inner beam pipe walls at FPM location was blackened to avoid reflections (b) the gas injection layout was optimized which includes, placing the gas dosing valve close to the beam line, using stainless steel pipes and connectors and placing the gas inlet in the opposite location of the pressure gauge. After this, measurements were improved by a factor of 10, thus pressures in the range of 10^{-5}-10^{-6} mbar were enough even for beam currents in the micro-Ampere range (Fig. 11b) [19].

Figure 11(a) shows the analysis of the beam position resolution during first experiments where 20 µm was achieved. A contour plot of the beam profiles recorded for 5µA, $8{\cdot}10^{-6}$ mbar, 50 ms acquisition time is shown in Fig. 11(b) and it is used as reference for extrapolations here. Beam steering experiments were performed (Fig. 11(c)) to demonstrate the beam tracking capabilities of FPMs and to analyze the beam position resolution achievable during a steered beam (Fig. 11(d)). A 50 µm resolution was achieved under such conditions. The experimental data is used for extrapolation to LIPAc conditions at the D-Plate location (10^{-7}mbar), showing the ability to measure beam profiles for pulses down to 14 µs for the PMT prototype (see Fig. 11b).

ISBN 978-3-95450-119-9

Profiler will be installed also close to the beam dump where the pressure grows up to 10^{-5} mbar, but radiation background is huge (> few tens Sv/h for neutrons). Therefore, due to its rather hard radiation behavior, the PMT solution will be retained instead of the CID. A different approach will be followed for profilers close to IFMIF targets comprising in decoupling the lens and detector with a 2D array of radiation hard fibers. The effect of high space charge on the beam profile measurement is currently being evaluated with promising results; in case of need, filters can be used.

Beam Loss Monitor (BLoM)

The BLoM system aims at protecting LIPAc against irremediable losses providing a fast interlock signal to the MPS in less than 10 µs. It also has to monitor the beam losses routinely.

Due to low beam energy, deuterons will be stopped inside the beam pipe generating secondary particles like neutrons and γ which can escape with an energy ranging from few keV up to 10 MeV.

Since reliability is a major concern, LHC-type ICs [20] were chosen. The nuclear reactions ^{56}Fe(D,n)X and ^{56}Fe(D,γ)X [21] were simulated to estimate IC current induced for 1W/m. Currents vary from 30 pA to 2 pA with beam axis distances going from 12 to 100 cm respectively. IC calibration campaigns with 3 and 14.7 MeV neutrons and 1.25 MeV γ were performed and the IC signal was found to be in good agreement with LHC calibration simulations. It should be stressed that the beam dump backscattering contribution can be huge compared to the 1W/m beam losses.

Figure 12 shows that integrating the signal over 200 ms is enough to separate 1 pA IC current; this measurement was done at Saclay on the ^{60}Co irradiator CoCase. For monitoring purposes, signals can be integrated over up to one second. Read-outs like transimpedances amplifiers, picoam-meter, and logarithmic amplifier have shown a good IC current linearity between 4 to 12 pA.

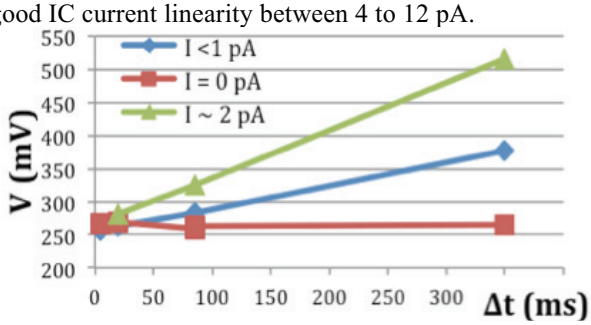

Figure 12: IC integration signal versus integration time for IC current.

The most important goal of BLoM system is the LIPAc security. MPS should be alerted in 10µs, requiring 20 µs more to stop the injector in emergency process. Assuming that one IC triggers the MPS when the current reaches 1nA, even if it is set at 1m from the beam axis (worst case), losses correspond to 500 W/m but only 15 mJ is deposited in 30 µs. Such a power deposition, even up to 1 J is not harmful for the accelerator.

Thus, Front-End Electronics will be designed to monitor losses by integrating over one second while discriminators, with various thresholds, will be implemented to trigger the MPS.

Micro Loss Monitor (µLoM)

This is a new type of monitors that results from a request of the Beam Dynamics team. Due to the very high space charge of the beam, dynamics group proposed to tune the beam by minimizing the beam halo instead of optimizing the beam core as it is usually done. This implies to detect very low beam losses (<10^{-6}).

Such monitors will be installed inside the cryomodule of the SRF Linac (8 ensembles made of 1 cavity, 1 solenoid and 1 BPM), close enough to the beam in order to have quite a good loss localization. Their requirements are:

- Good sensitivity to neutrons, but low for X-rays and γ. Indeed, the Linac superconductive cavities can emit numerous photons spreading from X-rays to γ range. These photons can induce fake signals mimicking beam losses,
- Good reliability: once closed the cryomodule will not be reopen,
- Ability to work at 4.5 K,
- Get a reasonable counting rate in one minute,
- Radiation hardness.

Single-crystalline CVD diamonds (Chemical Vapor Deposit) seem to be a good compromise [22]. It is planned to fix three diamonds on each solenoid, meaning a total of 24 diamonds. Reasonable longitudinal and azimuthal loss locations may be achieved with three diamonds and will improve the reliability by increased redundancy.

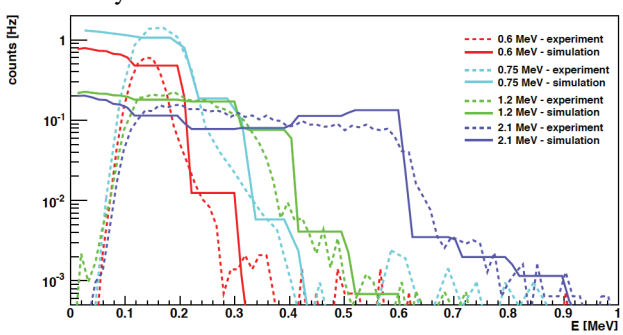

Figure 13: CVD diamond data for various neutron energies (experiment=dashed; theoretical=full line).

Neutron and γ counting rates were estimated with diamonds of 4×4×0.5 mm^3 (only 3×3 mm^2 active surface) and for 1 W/m losses in cw beam mode. For a threshold of 100 keV, 4.3 kHz events are expected, while the rate is only 2.7 kHz for a 200 keV threshold. Background contributions were estimated and were found to be reasonably low. Anyway, note that for 10^{-3} duty cycle, expected rates are 258 (162) counts/mn for 100 (200) keV thresholds.

Experimental neutron data were recorded at room temperature for 0.6, 0.75, 1.2 and 2.1 MeV neutron

ISBN 978-3-95450-119-9

energies. In Fig. 13, a good agreement with theoretical expectation (MCNPX 2.5 calculations using ENDF/B-V.0 library for ^{12}C and LLNL library for ^{13}C) is shown, relying on the previously estimated rates.

Slits

Slits are beam intercepting devices, thus very challenging design is required for low energy and high current beams. Three slits will be installed in LIPAc: two in the DP will be used for emittance measurements at 5 and 9 MeV. One of these DP slits together with an additional one implemented upstream the LIPAc dipole will be used for beam energy spread measurements, The first slit will be particularly tricky since it will have to handle roughly the entire beam pulse power. A proposed design for slit is shown on Fig. 14-left. It is based on the LINAC4 model but graphite has to be replaced, since, as already mentioned, it is forbidden for LIPAc. The concept relies on the use of blades of high fusion temperature material (refractory) to intercept the very high beam power density. The penetrating depth for deuterons in tungsten is 45μm at 5 MeV and 100μm at 9 MeV; hence the Bragg peak is very close to the blade surface. The blade should be in good thermal contact to a radiator to efficiently evacuate heat through water-cooling channels for instance. Sharper angles allow for spreading the deposited energy over a larger surface. At 9 MeV, the nominal beam shape leads to a huge surface power density of 1.5 GW/m^2.

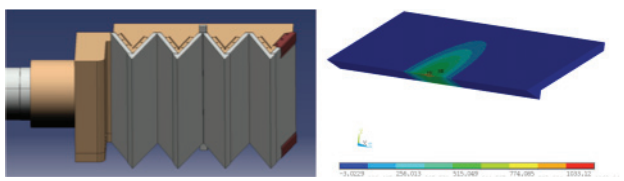

Figure 14: Design for a high power slit with a 100 μm aperture (left). Temperature distribution for a TZM blade at nominal beam conditions for a 100μs pulse length (right).

A thermo-mechanical study of the slit has been performed assuming a low duty cycle beam of 10^{-4} (100μs/s), which is divided in three stages:

- 1D (thickness) model for the study of main conduction effects and evaluation of thickness, materials and incidence angle.
- 2D transverse (plane strain) model for evaluation of conduction due to beam footprint gradients and studying the effects in the plate faces.
- 3D model for evaluation of thermal deformation on contact pressure, full conduction process, out of plane deformations, plastic behavior and support requirements.

Tungsten and TZM, a ductile molybdenum alloy, were investigated with 3 mm thickness and preliminary results show a preference for TZM at 15° incident angle. Results are very similar for those at 10° but larger angles are easier to manufacture. The deformation is limited to 10 μm, so it should not be a problem to maintain the thermal contact with the copper body.

A slit prototype was manufactured at CIEMAT Madrid to validate the very difficult thermal study.

Beam Profile Monitors (BPM)

The Beam Position and Phase Monitors for LIPAc [23] will become one of the key devices for the beam commissioning and operation of the accelerator. They will provide to the CCS (Central Control System) with the variation of the beam centroid in the transverse plane (position) and the longitudinal plane (phase). The BPMs will be distributed along the accelerator, in locations required by the beam dynamics team to provide a good feedback for steering and transporting the beam from the RFQ to the Beam Dump.

Several problems have to be overcome along the accelerator like:

- low β effect, which broadens the electromagnetic field accompanying the beam, which decreases the expected signal,
- beam de-bunching, particularly relevant in the last part of LIPAc,
- lack of space. For instance, BPMs must be embedded into quadruples at MEBT location,
- thermal conditions: special care has to be taken for BPMs inserted in the SRF Linac cryomodule,
- high radiation levels may concern the BPM design particularly for those close to the BD. The electronics has to be placed outside the vault, which represents up to 70 m distance between the sensor and the acquisition.

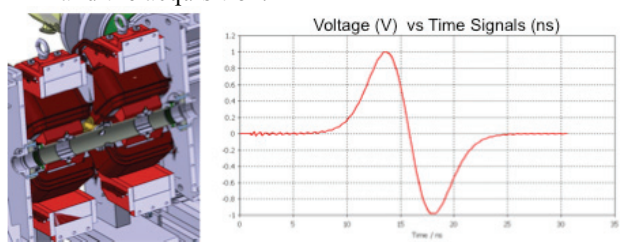

Figure 15: Two MEBT BPMs welded on the beam pipe and installed inside quadruples (left). Simulation of a button response for the last BPM (close to BD - right).

For these reasons, several types of BPMs with different concepts and sizes are in design progress, while only 17 are requested. Hereunder is a summary of them:

- Four BPMs for the MEBT [24] will be installed inside 4 of the 5 quadruples, in the middle of the vacuum section, to provide transversal beam position. Mechanical complexity to insert them in small space puts high constraints on the design (Fig. 15-left). Striplines are selected to minimize the thermal load in the electrical vacuum feedthroughs. A first prototype is under manufacturing.
- Eight cryogenic BPMs with buttons will be implemented in the cryostat of the SRF Linac (4.5 K). Buttons manufactured for the LHC BPM's have been selected. Coaxial cable design is also very

ISBN 978-3-95450-119-9

delicate due to stringent electrical and thermal specifications. Read-out will be done on the second harmonic to avoid RF signal from HWR cavities.

- Three striplines will be set in the D-Plate to measure the beam energy using the time of flight technique. Shorted striplines are chosen for the mechanical robustness. With the present distance of around 1.2 m between BPM's, the energy beam resolution may vary from 0.03% to 0.25% for phase resolution of 0.1°, 2° respectively. Such a stripline BPM is in manufacturing progress in CIEMAT Madrid workshop.
- BPM for the HEBT will be made with cylindrical electrodes of diameters 40, 130 and 150 mm. For the BPM close to the BD, de-bunching is quite important, but simulations have shown that signal is high enough at the fundamental frequency of observation (Fig. 15-right). In that case the electrode length is about 80 mm.

The BPM's are characterized in a special wire test bench [25] before installation in the machine.

Regarding the acquisition electronics, CIEMAT is developing a prototype based on IQ demodulation of the first or second harmonic of the BPM's signal. The prototype will include an automatic calibration procedure to minimize phase and amplitude errors in the long cables between the LIPAC and the vault.

Bunch Length Monitor

This monitor is a non interceptive device based on a former GSI development [26]. A homogeneous electric field is placed between two plates set inside the beam pipe (see Fig. 16). Electrons produced by ionization of the residual gas by the beam are collected towards one of this plate where a slit system is used to collimate this secondary electron beam. This later encounters then a bending electric field to select electrons with a specific energy (electro-static analyser). This guaranties that electrons have similar traveling time wherever they were emitted.

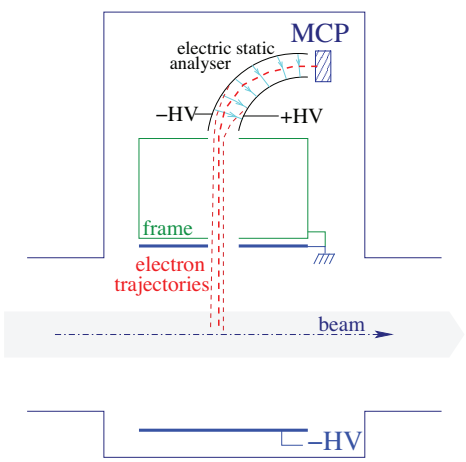

Figure 16: BLM principle developed by INFN.

Finally electrons are driven to a Multi Channel Plate (MCP) where their time of flight versus the RF phase is measured. This later step was implemented by INFN Legnaro group while a time-to-spatial transformation was performed with a RF-deflector in the GSI prototype [27].

Therefore the multiplied electrons are collected through 50 Ω anode of the MCP. The time coincidence between this signal and the master oscillator gives the time bunch length (Start-Stop technique).

A RGBLM (Residual Gas Bunch Length Monitor) prototype was carried out and tested at the INFN Legnaro National labs (LNL) accelerators using several beams (unfortunately not protons or deuterons) for various energies, current and timing conditions. The aperture of the BLM was 50×50 mm^2 and 70 mm as longitudinal size while the gap between analysing plates was 10 mm with a mean bending radius of 30 mm. Resolution capabilities were measured and improved during test campaigns to achieve 300 ps FWHM for a $^{136}Xe^{28+}$ beam at 546 MeV from the RFQ+LINAC accelerators at 40 MHz RF (see Fig. 17).

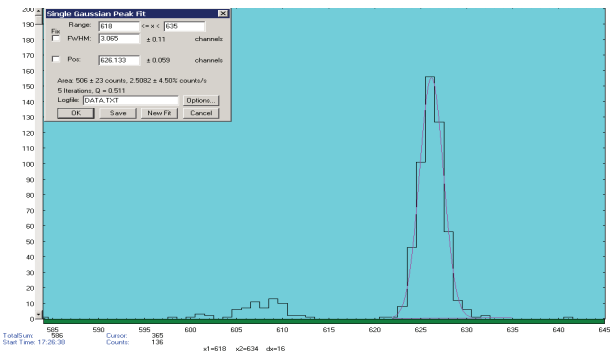

Figure 17: $^{136}Xe^{28+}$ at 546 MeV. Resolution is about 300 ps FWHM.

A new prototype with an aperture of 100×100 mm^2 is under progress to fulfill the BSC required by beam dynamics group.

CONCLUSION

LIPAc is a very ambitious project with challenges never faced before in particle accelerators, namely the combination of high power, high intensity, strong space charge and high radiation background. All those have great impact on the accelerator design.

This article gives an overview of the beam diagnostics, which have been foreseen to operate gradually from low beam intensity and duty cycle towards cw beam.

After a LIPAc diagnostic overview, some particularly challenging diagnostics are depicted in more details focusing on tests or strategies taken to overcome them. The diagnostics design phase is almost completed, whilst electronics and control command still requires further development. For diagnostics downstream to the RFQ, the next important step is the RFQ commissioning, which is schedule for summer 2015.

ISBN 978-3-95450-119-9

ACKNOWLEDGMENT

Authors would like to thank the GSI beam diagnostics group, the IPHI team at Saclay, the CoCase group at Saclay, the beam dynamics group, the Centro Nacional de Aceleradores at Sevilla, B. Dehning at CERN who gave us an IC and advises and CERN beam diagnostics group.

CIEMAT Madrid contributions have been partially funded by the MINECO Ministry under projects AIC10-A-000441 and AIC-A-2011-0654.

REFERENCES

[1] IFMIF Comprehensive Design Report. http://www.iea.org/techno/technologies/fusion/IFMIF-CDR_partA.pdf

[2] K. Ehrlich and A. Möslang, IFMIF "An international fusion materials irradiation facility", NIM in Physics Research B139, 72–81,998.

[3] A. Mosnier et al., "The accelerator prototype of the IFMIF-EVEDA project", in Proceedings of IPAC'10, Kyoto, Japan.

[4] P. A. P Nghiem et al., "The IFMIF-EVEDA challenges in beam dynamics and their treatment", NIM in Physics Research A654, 63–71, 2011.

[5] R. Gobin et al., "Preliminary results of the international fusion materials irradiation facility deuteron injector", Review of scientific instruments, 83:02A345–1 – 4, 2012.

[6] A. Pisent et al., "IFMIF-EVEDA RFQ design", In Proc. of EPAC08, Genua, Italy, 2008.

[7] F. Orsini et al., "Preliminary results of the IFMIF cavity prototypes tests in vertical cryostat and cryomodule development", in Proc. of SRF2011, Chicago, IL, USA, 2011.

[8] B. Brañas et al., "Design of a Beam Dump for the IFMIF-EVEDA accelerator", Fusion Engineering and Design84 (2009) 509-513.

[9] E. Delagnes, Private communication.

[10] F. Senée et al., "Diagnostics for high power ion beams with coherent optic fiber for IFMIF-EVEDA injector", in Proceedings DIPAC11, Hamburg, Germany.

[11] R. Gobin et al., "Light ion ECR sources state of the art for Linacs", in Proceedings Linac12, Tel Aviv, Israel.

[12] J.L. Vignet et al., in Proceedings DIPAC09, Basel.

[13] COMSOL software, http://www.comsol.com/

[14] J. Egberts et al., "detailed experimental characterization of an ionization profile monitor", in Proceedings of DIPAC11, Hamburg, Germany.

[15] Lorentz, http://www.integratedsoft.com/

[16] Jan Egberts, PhD thesis "IFMIF-LIPAc Beam Diagnostics: Profiling and Loss Monitoring Systems" (available soon), September 25th, 2012.

[17] P.Y. Beauvais et al., "Installation of the French high-intensity proton injector at Saclay", Linac 2006, Knoxville, August 2006, 153.

[18] JM Carmona et al., Phys. Rev. ST Accel. Beams **15**, 072801 (2012).

[19] J.M. Carmona et al., "New tests of fluorescence beam profilers for the linear IFMIF prototype accelerator (LIPAc) using 9 MeV deuteron beams". Proceedings of the BIW'12, TUPG028. Newport News, USA (2012). ISBN 978-3-95450-121-2.

[20] M. Sapinski et al., "Response functions of ionization chamber beam loss monitor". Technical report, CERN, 2010.

[21] Talys & MCNPX, September 2010.

[22] M. Angelone et al., "Neutron detectors based upon artificial single crystal diamond", IIE Transactions on Nuclear Science, Vol. 56, n°4, August 2009.

[23] I. Podadera et al., "Design status of BPMs for the IFMIF-EVEDA accelerator", in Proceedings of DIPAC09, Basel, Switzerland.

[24] I. Podadera, "Developments for IFMIF/EVEDA LIPAC Beam Position Monitors: the sensor at the MEBT and the wire test bench", in Proceedins of DIPAC'11.

[25] C. Boccard, Proceedings of CARE Workshop, Lueneburg, Germany (2007).

[26] P. Fork et al., "Measurements with a novel non-intercepting Bunch Shape Monitor at the high current GSI-Linac", in Proceedings of DIPAC'05.

[27] A.V. Feschenko, "Methods and instrumentation for Bunch Shape Measuremùent", in Proceedings of PAC 2001, Chicago, USA.

ISBN 978-3-95450-119-9